Korean J. Chem. Eng., **25**(1), 41-45 (2008)

Effect of Al_2O_3-ZrO_2 xerogel support on hydrogen production by steam reforming of LNG over Ni/Al_2O_3-ZrO_2 catalyst

Jeong Gil Seo, Min Hye Youn, Kyung Min Cho, Sunyoung Park, Sang Hee Lee, Joohyung Lee and In Kyu Song†

School of Chemical and Biological Engineering, Research Center for Energy Conversion and Storage, Seoul National University, Shinlim-dong, Gwanak-gu, Seoul 151-744, Korea
(*Received 3 April 2007 • accepted 11 June 2007*)

Abstract−An Al_2O_3-ZrO_2 xerogel (AZ-SG) was prepared by a sol-gel method for use as a support for a nickel catalyst. The Ni/AZ-SG catalyst was then prepared by an impregnation method, and was applied to hydrogen production by steam reforming of LNG. A nickel catalyst supported on commercial alumina (A-C) was also prepared (Ni/A-C) for comparison. The hydroxyl-rich surface of the AZ-SG support increased the dispersion of nickel species on the support during the calcination step. The formation of a surface nickel aluminate-like phase in the Ni/AZ-SG catalyst greatly enhanced the reducibility of the Ni/AZ-SG catalyst. The ZrO_2 in the AZ-SG support increased the adsorption of steam onto the support and the subsequent spillover of steam from the support to the active nickel sites in the Ni/AZ-SG catalyst. Both the high surface area and the well-developed mesoporosity of the Ni/AZ-SG catalyst improved the gasification of adsorbed surface hydrocarbons in the reaction. In the steam reforming of LNG, the Ni/AZ-SG catalyst showed a better catalytic performance than the Ni/A-C catalyst. Moreover, the Ni/AZ-SG catalyst showed strong resistance toward catalyst deactivation.

Key words: Al_2O_3-ZrO_2 Xerogel, Sol-gel, Supported Nickel Catalyst, Steam Reforming, LNG, Hydrogen Production

INTRODUCTION

Hydrogen has attracted much attention as a promising energy due to its clean, renewable, and non-polluting nature. Technological advances in fuel cells have made hydrogen more important as a new energy source [1-3]. A number of catalytic reforming technologies have been developed for hydrogen production from hydrocarbons [4-10]. Among the reforming technologies, steam reforming of methane has been recognized as a feasible route to producing hydrogen. LNG, which is abundant and mainly composed of methane, can serve as an alternate source for hydrogen production by steam reforming. The extensive piping system of LNG in modern cities also makes LNG well suited as a hydrogen source for residential reformers in fuel cell applications.

Nickel-based catalysts have been widely used in the steam reforming reactions. However, they require a high reaction temperature and an excess amount of steam to prevent the coke deposition on the catalyst surfaces [5,11]. Furthermore, the supported nickel catalysts operated at high temperatures show a strong metal-support interaction, inhibiting the reduction of nickel species into the active metallic nickel [12,13]. Developing an efficient catalyst with high activity and high durability is therefore required for hydrogen production in low temperature steam reforming reactions. Although noble metals are known to be very active in the steam reforming reactions, the nickel-based catalysts can be a practical candidate if properly designed.

Supported nickel catalysts generally suffer from severe catalyst deactivation due to the carbon deposition on the catalyst surface, the sintering of nickel particles, and the insufficient thermal and chemical stability of the supporting material. A number of attempts have been made to overcome these problems. For example, it was reported that the addition of second metals such as molybdenum, magnesium, calcium, potassium, cerium, and zirconium into the supported nickel catalysts enhanced the catalytic performance in the steam reforming reactions [14-19]. Ni-Al_2O_3 catalysts prepared by a sol-gel method [20-23] were also investigated in the reforming reactions with the aim of suppressing the carbon deposition [24-26]. It is known that metal oxides prepared by a sol-gel method have high surface areas and unique textural and chemical properties. Therefore, developing a sol-gel derived metal oxide support for a nickel catalyst in hydrogen production by steam reforming of LNG would be of great interest.

In this work, an Al_2O_3-ZrO_2 xerogel was prepared by a sol-gel method for use as a support for a nickel catalyst. Ni/Al_2O_3-ZrO_2 catalyst was then prepared by an impregnation method, and was applied to hydrogen production by steam reforming of LNG. The effect of Al_2O_3-ZrO_2 xerogel support on the catalytic performance of Ni/Al_2O_3-ZrO_2 in the steam reforming of LNG was investigated.

EXPERIMENTAL

1. Preparation of Al_2O_3-ZrO_2 Xerogel Support and Ni/Al_2O_3-ZrO_2 Catalyst

An Al_2O_3-ZrO_2 xerogel support was prepared by a sol-gel method, according to a similar method reported in the literature [24,26,27]. Known amounts of aluminum precursor (aluminum *sec*-butoxide, Sigma-Aldrich) and zirconium precursor (zirconium *tert*-butoxide, Sigma-Aldrich) were dissolved in ethanol at 80 °C with vigorous stirring for uniform dispersion of each precursor. Small amounts of

†To whom correspondence should be addressed.
E-mail: inksong@snu.ac.kr

distilled water and nitric acid, which had been diluted with ethanol, were slowly added into a solution containing aluminum and zirconium precursors for the partial hydrolysis of each precursor. After the resulting solution was maintained at 80 °C for a few minutes, a clear sol was obtained. The sol was then cooled to room temperature with constant stirring. A transparent monolithic gel was formed within a few minutes by adding an appropriate amount of water diluted with ethanol into the sol. After aging the Al_2O_3-ZrO_2 gel for 24 h, it was dried overnight at 120 °C. The resulting powder was finally calcined at 700 °C for 5 h to yield the Al_2O_3-ZrO_2 xerogel support. The prepared Al_2O_3-ZrO_2 xerogel support was denoted as AZ-SG.

A nickel catalyst supported on AZ-SG was prepared by impregnating a known amount of nickel precursor ($Ni(NO_3)_2 \cdot 6H_2O$, Sigma-Aldrich) onto the AZ-SG. The prepared Ni/Al_2O_3-ZrO_2 catalyst was denoted as Ni/AZ-SG. For comparison, a nickel catalyst supported on commercial Al_2O_3 (Degussa, denoted as A-C) was also prepared by an impregnation method. The nickel catalyst supported on commercial Al_2O_3 was denoted as Ni/A-C. The nickel loading was fixed at 20 wt% in both cases.

2. Characterization

Chemical compositions of AZ-SG support and Ni/AZ-SG catalyst were determined by ICP-AES analyses (Shimadzu, ICPS-1000IV). Nitrogen adsorption-desorption isotherms were obtained with an ASAP-2010 (Micromeritics) instrument, and pore size distributions were determined by the Barret-Joyner-Hallender (BJH) method applied to the desorption branch of the nitrogen isotherm. Carbon deposition on the supported catalysts was examined by TEM analyses (Jeol, JEM-2000EXII). Crystalline phases of supports and supported catalysts were investigated by XRD (MAC Science, M18XHF-SRA) measurements by using Cu-Kα radiation (λ=1.54056 Å) operated at 50 kV and 100 mA. In order to examine the reducibility of supported catalysts, temperature-programmed reduction (TPR) measurements were carried out in a conventional flow system with a moisture trap connected to a thermal conductivity detector (TCD) at temperatures ranging from room temperature to 1,000 °C with a ramping rate of 5 °C/min. For the TPR measurements, a mixed stream of H_2 (2 ml/min) and N_2 (20 ml/min) was used for 0.1 g of catalyst sample.

3. Steam Reforming of LNG

The steam reforming of LNG was carried out in a continuous flow fixed-bed reactor at atmospheric pressure. Each calcined catalyst (100 mg) was charged into a tubular quartz reactor, and it was then reduced with a mixed stream of H_2 (3 ml/min) and N_2 (30 ml/min) at 700 °C for 3 h. Water was sufficiently vaporized by passing through a pre-heating zone and continuously fed into the reactor together with LNG (92 vol% CH_4 and 8.0 vol% C_2H_6) and N_2 carrier (30 ml/min). The steam/carbon ratio in the feed stream was fixed at 2.0, and the total feed rate with respect to the catalyst was maintained at 27,000 ml·h^{-1}g^{-1}. The catalytic reaction was carried out at 600 °C. The reaction products were periodically sampled and analyzed by using an on-line gas chromatograph (Younglin, ACME 6000) equipped with a thermal conductivity detector. LNG conversion and hydrogen composition in dry gas were calculated according to the following equations.

$$\text{LNG conversion } (\%) = \left(1 - \frac{F_{CH_4,out} + F_{C_2H_6,out}}{F_{CH_4,in} + F_{C_2H_6,in}}\right) \times 100$$

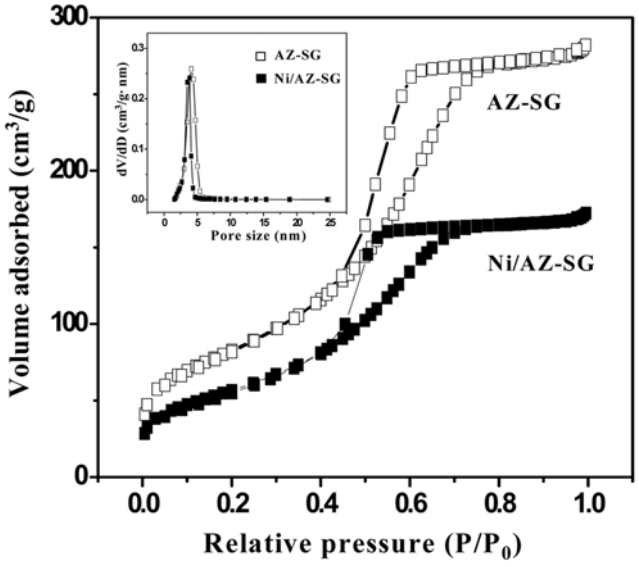

Fig. 1. Nitrogen adsorption-desorption isotherms and pore size distributions of AZ-SG support and Ni/AZ-SG catalyst.

$$\text{Hydrogen composition in dry gas } (\%) = \frac{F_{H_2,out}}{F_{H_2,out} + F_{CH_4,out} + F_{C_2H_6,out} + F_{CO,out} + F_{CO_2,out}} \times 100$$

RESULTS AND DISCUSSION

1. Textural and Chemical Properties of Supports and Supported Ni Catalysts

Fig. 1 shows the nitrogen adsorption-desorption isotherms and pore size distributions of AZ-SG support and Ni/AZ-SG catalyst. Both AZ-SG support and Ni/AZ-SG catalyst clearly showed the IV-type isotherms with H_2 hysteresis loops, indicating the existence of well-developed mesopores. The average pore sizes were found to be 3.8 nm for AZ-SG support and 3.4 nm for Ni/AZ-SG catalyst. Detailed textural and chemical properties of supports (A-C and AZ-SG) and supported Ni catalysts (Ni/A-C and Ni/AZ-SG) are listed in Table 1. The Zr/Al atomic ratio in both AZ-SG support and Ni/AZ-SG catalyst was 0.15. The AZ-SG support had a higher surface area and a larger pore volume than the A-C support. Moreover, the Ni/AZ-SG catalyst retained a higher surface area and a

Table 1. Textural and chemical properties of supports (A-C and AZ-SG) and supported Ni catalysts (Ni/A-C and Ni/AZ-SG)

Sample	Surface area (m^2/g)[a]	Pore volume (cm^3/g)[b]	Average pore size (nm)[c]	Zr/Al atomic ratio[d]
A-C	95	0.25	12.5	-
AZ-SG	300	0.43	3.8	0.15
Ni/A-C	82	0.30	17.0	-
Ni/AZ-SG	206	0.32	3.4	0.15

[a]Calculated by the BET equation.
[b]BJH desorption pore volume.
[c]BJH desorption average pore diameter.
[d]Determined by ICP-AES analysis.

larger pore volume than the Ni/A-C catalyst. The Ni/AZ-SG catalyst showed a lower surface area and a smaller pore volume than the AZ-SG support, due to the pore blocking by nickel species occurred during the impregnation step. However, the Ni/A-C catalyst showed a larger pore volume and a larger pore size than the A-C support. This can be explained by the action of the nickel species. The nickel species employed in the impregnation step play a role of forming large textural pores by aggregating non-porous nanoparticles of A-C [28].

2. Crystalline Structures of Supports and Supported Ni Catalysts

Fig. 2 shows the XRD patterns of A-C and AZ-SG supports calcined at 700 °C for 5 h. The A-C support showed the typical diffraction peaks of γ-Al_2O_3. However, the AZ-SG support showed no characteristic diffraction peaks of either alumina or zirconia. This indicates that the homogeneous mixing between alumina and zirconia occurred in the preparation of AZ-SG support, resulting in the formation of amorphous Al_2O_3-ZrO_2 composite structure. It is

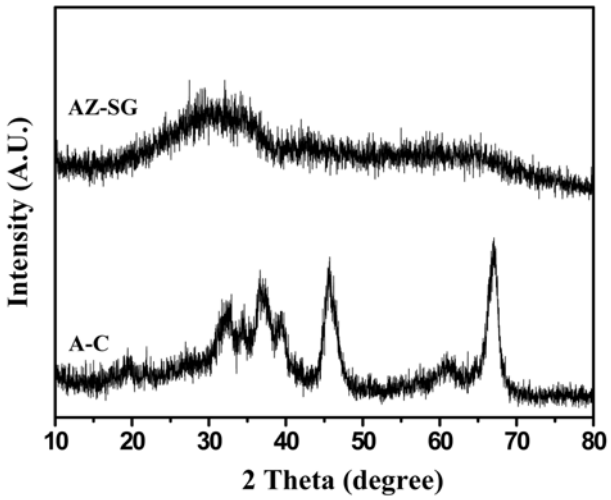

Fig. 2. XRD patterns of A-C and AZ-SG supports calcined at 700 °C for 5 h.

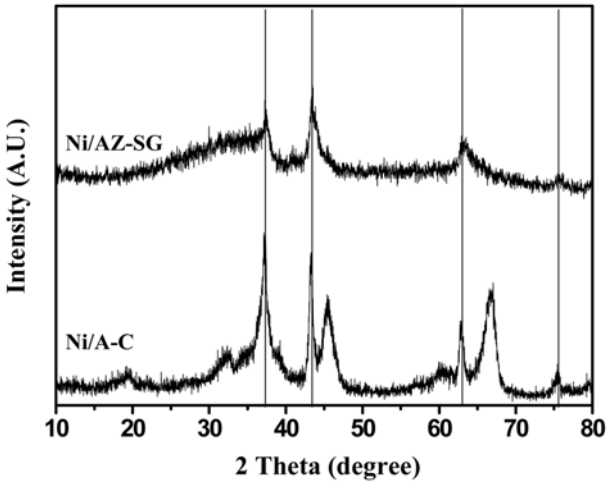

Fig. 3. XRD patterns of Ni/A-C and Ni/AZ-SG catalysts calcined at 700 °C for 5 h.

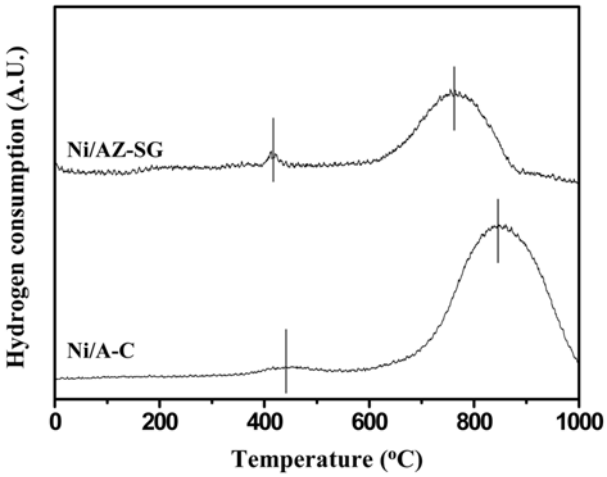

Fig. 4. TPR profiles of Ni/A-C and Ni/AZ-SG catalysts.

believed that the hydroxyl-rich surface properties of the AZ-SG retarded the aggregation of Al_2O_3 and ZrO_2 particles even after the heat treatment at high temperature.

Fig. 3 shows the XRD patterns of Ni/A-C and Ni/AZ-SG catalysts calcined at 700 °C for 5 h. Solid lines represent the nickel oxide species on the catalysts. Both nickel oxide and nickel aluminate-like species were observed in the Ni/A-C catalyst. The existence of nickel aluminate-like species was confirmed by the shift of diffraction peak of γ-Al_2O_3, as reported in the literature [29,30]. On the other hand, the Ni/AZ-SG catalyst showed broader diffraction peaks of nickel species than the Ni/A-C catalyst. This result indicates that the nickel species were finely dispersed in the Ni/AZ-SG catalyst by forming small particles. It is believed that the hydroxyl-rich surface of the AZ-SG support played an important role in forming highly dispersed nickel species in the Ni/AZ-SG catalyst.

3. Reducibility of Ni/A-C and Ni/AZ-SG Catalysts

Fig. 4 shows the TPR profiles of Ni/A-C and Ni/AZ-SG catalysts. The minor reduction bands appearing at low temperature in both catalysts are attributed to the reduction of bulk nickel oxide species. The major reduction band appearing at around 820 °C in the Ni/A-C catalyst is due to the reduction of bulk nickel aluminate-like phase, while that appearing at around 750 °C in the Ni/AZ-SG catalyst is due to the reduction of surface nickel aluminate-like phase. It is believed that both the mesoporosity and the hydroxyl-rich surface of the AZ-SG support induced the formation of surface nickel aluminate-like phase in the Ni/AZ-SG catalyst. It is known that the surface nickel aluminate phase is much easier to reduce than the bulk nickel aluminate phase [31-33]. It is also inferred that the small amount of ZrO_2 weakened the interaction between nickel species and support through the formation of favorable Al_2O_3-ZrO_2 composite structure in the Ni/AZ-SG catalyst. The above results indicate that the Ni/AZ-SG catalyst retained higher reducibility than the Ni/A-C catalyst.

4. Steam Reforming of LNG over Ni/A-C and Ni/AZ-SG Catalysts

Fig. 5 shows the LNG conversions with time on stream in the steam reforming of LNG over Ni/A-C and Ni/AZ-SG catalysts at 600 °C. The Ni/A-C catalyst showed a rapid catalyst deactivation, whereas the Ni/AZ-SG catalyst showed a stable catalytic perfor-

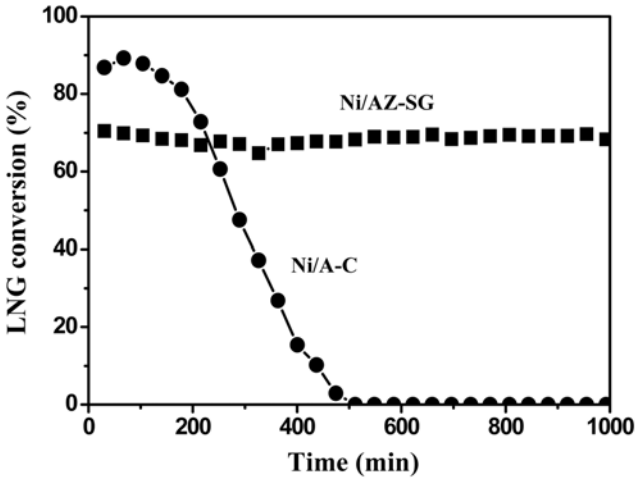

Fig. 5. LNG conversions with time on stream in the steam reforming of LNG over Ni/A-C and Ni/AZ-SG catalysts at 600 °C.

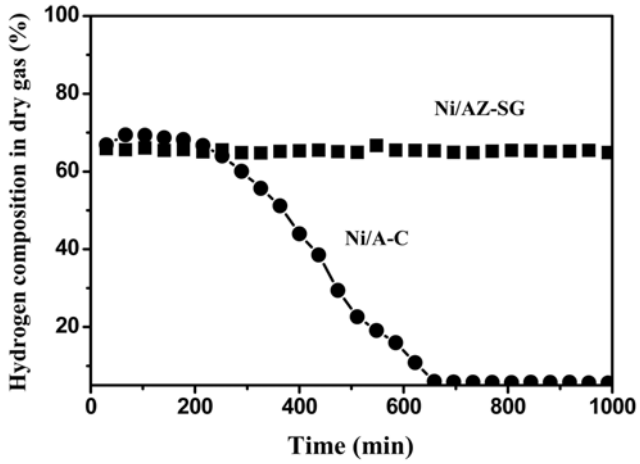

Fig. 7. Hydrogen compositions in dry gas with time on stream in the steam reforming of LNG over Ni/A-C and Ni/AZ-SG catalysts at 600 °C.

mance during the reaction extending over 1,000 min. This result can be explained by the chemical and textural properties of the AZ-SG support. One possible reason is the high reducibility of the Ni/AZ-SG catalyst (Fig. 4). It is likely that the hydroxyl-rich surface of the AZ-SG support enhanced the dispersion of nickel species through the formation of a surface nickel aluminate-like phase in the Ni/AZ-SG catalyst. It is also believed that the highly dispersed zirconia in the AZ-SG support increased the adsorption of steam onto the support and the subsequent spillover of steam from the support to the active nickel sites [19,34]. Another possible reason for the enhanced catalytic performance of Ni/AZ-SG may be due to the favorable textural structure of the AZ-SG support. Both the high surface area and the well-developed mesoporosity of the Ni/AZ-SG catalyst effectively suppressed the carbon deposition, and at the same time, enhanced the gasification of adsorbed hydrocarbons in the reaction.

Fig. 6 shows the TEM images of Ni/A-C and Ni/AZ-SG catalysts after a 1,000-min reaction. The used Ni/A-C catalyst showed the filamentous carbon. CHNS elemental analyses revealed that the used Ni/A-C catalyst contained 12 wt% carbon species after a 1,000-min reaction. On the other hand, the used Ni/AZ-SG catalyst showed no distinguishable filamentous carbon, and only a small amount of carbon species (0.8 wt%) was deposited on the Ni/AZ-SG catalyst even after a 1,000-min reaction. Furthermore, the Ni/AZ-SG catalyst showed no significant sintering of nickel particles compared to the Ni/A-C catalyst. It is believed that the highly dispersed small nickel particles on the Ni/AZ-SG catalyst are responsible for strong resistance toward carbon deposition in the steam reforming of LNG.

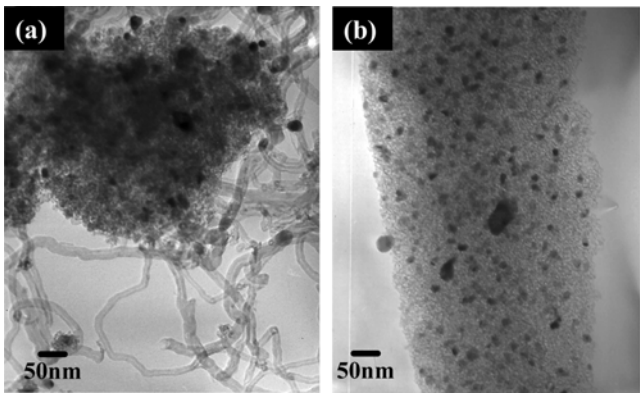

Fig. 6. TEM images of (a) Ni/A-C and (b) Ni/AZ-SG catalysts after a 1,000-min reaction.

Fig. 7 shows the hydrogen compositions in dry gas with time on stream in the steam reforming of LNG over Ni/A-C and Ni/AZ-SG catalysts at 600 °C. The hydrogen compositions showed a similar trend to the LNG conversions (Fig. 5) over both catalysts. The Ni/AZ-SG catalyst produced ca. 70% hydrogen (dry gas basis), a slightly lower value than the theoretical estimate (75%). It is concluded that the AZ-SG support prepared by a sol-gel method served as an efficient support for the nickel catalyst in hydrogen production by steam reforming of LNG.

CONCLUSIONS

The effect of AZ-SG support on the catalytic performance of Ni/AZ-SG catalyst was investigated. For comparison, a nickel catalyst supported on commercial alumina (A-C) was also prepared (Ni/A-C). It was found that the hydroxyl-rich surface of the AZ-SG support enhanced the dispersion of nickel species on the support through the formation of a surface nickel aluminate-like phase. The surface nickel aluminate-like phase of the Ni/AZ-SG catalyst improved the reducibility of the catalyst. In hydrogen production by steam reforming of LNG, the Ni/AZ-SG catalyst showed a better catalytic performance than the Ni/A-C catalyst. A small amount of ZrO_2 in the AZ-SG support enhanced the steam adsorption capability of the supported catalyst through the formation of a favorable Al_2O_3-ZrO_2 composite structure. Both the high surface area and the well-developed mesoporosity of the Ni/AZ-SG catalyst improved the gasification of adsorbed surface hydrocarbons in the reaction. It was also revealed that the Ni/AZ-SG catalyst showed strong resistance toward catalyst deactivation. It is concluded that the AZ-SG support prepared by a sol-gel method can serve as an efficient support

for the nickel catalyst in hydrogen production by steam reforming of LNG.

ACKNOWLEDGMENTS

The authors wish to acknowledge support from the Seoul Renewable Energy Research Consortium (Seoul R & BD Program) and RCECS (Research Center for Energy Conversion and Storage: R11-2002-102-00000-0).

REFERENCES

1. D. J. Moon, J. W. Ryu, S. D. Lee and B. S. Ahn, *Korean J. Chem. Eng.*, **19**, 921 (2002).
2. B.-G. Park, *Korean J. Chem. Eng.*, **21**, 782 (2004).
3. Q. Ming, T. Healey, L. Allen and P. Irving, *Catal. Today*, **77**, 51 (2002).
4. K. H. Kim, S. Y. Lee and K. J. Yoon, *Korean J. Chem. Eng.*, **23**, 356 (2006).
5. J. K. Lee and D. Park, *Korean J. Chem. Eng.*, **15**, 658 (1998).
6. S. W. Nam, S. P. Yoon, H. Y. Ha, S.-A. Hong and A. P. Maganyuk, *Korean J. Chem. Eng.*, **17**, 288 (2000).
7. J. Zhang, Y. Wang, R. Ma and D. Wu, *Korean J. Chem. Eng.*, **20**, 288 (2003).
8. A. Praharso, A. Adesina, D. L. Trimm and N. W. Cant, *Korean J. Chem. Eng.*, **20**, 468 (2003).
9. E. Promaros, S. Assabumrungrat, N. Laosiripojana, P. Praserthdam, T. Takawa and S. Goto, *Korean J. Chem. Eng.*, **24**, 44 (2007).
10. S. J. Kong, J. H. Jun and K. J. Yoon, *Korean J. Chem. Eng.*, **21**, 793 (2004).
11. J. N. Armor, *Appl. Catal. A*, **176**, 159 (1999).
12. H.-S. Roh, K.-W. Jun and S.-E. Park, *Appl. Catal. A*, **251**, 275 (2003).
13. A. Vargas, C. Maldonado, J. A. Montoya, L. Norena and J. Morales, *Appl. Catal. A*, **273**, 269 (2004).
14. T. Borowiecki, A. Golebiowski and B. Stasinska, *Appl. Catal. A*, **153**, 141 (1997).
15. T. Borowiecki, G. Wojciech and D. Andrzej, *Appl. Catal. A*, **270**, 27 (2004).
16. J. S. Lisboa, D. C. R. M. Santos, F. B. Passos and F. B. Noronha, *Catal. Today*, **101**, 15 (2005).
17. S. Natesakhawat, R. B. Watson, X. Wang and U. S. Ozkan, *J. Catal.*, **234**, 496 (2005).
18. H.-S. Roh, K.-W. Jun, W.-S. Dong, J.-S. Chang, S.-E. Park and Y.-I. Joe, *J. Mol. Catal. A*, **181**, 137 (2002).
19. J. G. Seo, M. H. Youn and I. K. Song, *J. Mol. Catal. A*, **268**, 9 (2007).
20. Y. Kim, P. Kim, C. Kim and J. Yi, *Korean J. Chem. Eng.*, **22**, 321 (2005).
21. T. V. Choudhary, C. Sivadinarayana and D. W. Goodman, *Chem. Eng. J.*, **93**, 69 (2003).
22. S. Tang, L. Ji, J. Lin, H. C. Zeng, K. L. Tan and K. Li, *J. Catal.*, **194**, 424 (2000).
23. A. Valentini, N. L. V. Carreno, L. F. D. Probst, E. R. Leite and E. Longo, *Micro. Meso. Mater.*, **68**, 151 (2004).
24. J.-H. Kim, D. J. Suh, T.-J. Park and K.-L. Kim, *Appl. Catal. A*, **197**, 191 (2000).
25. Y. Zhang, G. Xiong, S. Sheng and W. Yang, *Catal. Today*, **63**, 517 (2000).
26. D. J. Suh, T.-J. Park, J.-H. Kim and K.-L. Kim, *J. Non-Cryst. Solids*, **225**, 168 (1998).
27. D. J. Suh, T.-J. Park, J.-H. Kim and K.-L. Kim, *Chem. Mater.*, **9**, 1903 (1997).
28. P. Kim, Y. Kim, H. Kim, I. K. Song and J. Yi, *Appl. Catal. A*, **272**, 157 (2004).
29. A. Corma, V. Fornes, R. M. Aranda and F. Rey, *J. Catal.*, **134**, 58 (1992).
30. J. A. Wang, A. Morales, X. Bokhimi and O. Novaro, *Chem. Mater.*, **11**, 308 (1999).
31. M. L. Jacono, M. Schiavello and A. Cimino, *J. Phys. Chem.*, **75**, 1044 (1971).
32. S. Narayanan and K. Uma, *J. Chem. Soc. Faraday Trans.*, **81**, 273 (1983).
33. A. N. Kharat, P. Pendleton, A. Badalyan, M. Abedini and M. M. Amini, *J. Catal.*, **205**, 7 (2002).
34. Y. Matsumura and T. Nakamori, *Appl. Catal. A*, **258**, 107 (2004).